THE JOURNAL OF BIOLOGICAL CHEMISTRY VOL. 285, NO. 2, pp. 1138–1146, January 8, 2010
© 2010 by The American Society for Biochemistry and Molecular Biology, Inc. Printed in the U.S.A.

Functional Analysis of an *Arabidopsis thaliana* Abiotic Stress-inducible Facilitated Diffusion Transporter for Monosaccharides*[S]

Received for publication, August 10, 2009, and in revised form, November 6, 2009 Published, JBC Papers in Press, November 9, 2009, DOI 10.1074/jbc.M109.054288

Kohji Yamada[‡§], Yuriko Osakabe[‡], Junya Mizoi[§], Kazuo Nakashima[§], Yasunari Fujita[§], Kazuo Shinozaki[¶], and Kazuko Yamaguchi-Shinozaki[‡§1]

From the [‡]Laboratory of Plant Molecular Physiology, Graduate School of Agricultural and Life Sciences, The University of Tokyo, Tokyo 113-8657, Japan, the [§]Biological Resources Division, Japan International Research Center for Agricultural Sciences, Tsukuba, Ibaraki 305-8686, Japan, and the [¶]RIKEN Plant Science Center, Yokohama, Kanagawa 203-0045, Japan

Sugars play indispensable roles in biological reactions and are distributed into various tissues or organelles via transporters in plants. Under abiotic stress conditions, plants accumulate sugars as a means to increase stress tolerance. Here, we report an abiotic stress-inducible transporter for monosaccharides from *Arabidopsis thaliana* that is termed ESL1 (ERD six-like 1). Expression of *ESL1* was induced under drought and high salinity conditions and with exogenous application of abscisic acid. Promoter analyses using β-glucuronidase and green fluorescent protein reporters revealed that *ESL1* is mainly expressed in pericycle and xylem parenchyma cells. The fluorescence of ESL1-green fluorescent protein-fused protein was detected at tonoplast in transgenic *Arabidopsis* plants and tobacco BY-2 cells. Furthermore, alanine-scanning mutagenesis revealed that an N-terminal L*XXX*LL motif in ESL1 was essential for its localization at the tonoplast. Transgenic BY-2 cells expressing mutated ESL1, which was localized at the plasma membrane, showed an uptake ability for monosaccharides. Moreover, the value of K_m for glucose uptake activity of mutated ESL1 in the transgenic BY-2 cells was extraordinarily high, and the transport activity was independent from a proton gradient. These results indicate that ESL1 is a low affinity facilitated diffusion transporter. Finally, we detected that vacuolar invertase activity was increased under abiotic stress conditions, and the expression patterns of vacuolar invertase genes were similar to that of *ESL1*. Under abiotic stress conditions, ESL1 might function coordinately with the vacuolar invertase to regulate osmotic pressure by affecting the accumulation of sugar in plant cells.

In plants, sugars play essential roles as a main energy source, substrates for polymer synthesis, storage compounds, and carbon precursors that are required for a wide number of anabolic and catabolic reactions. To distribute sugars within whole plants, several transporters are required not only to traverse biological membranes on the subcellular level but also for long distance transport (1, 2). In most plant species, soluble sugars are mainly present in the forms of glucose, fructose, and sucrose. Sucrose is directly transported into sink cells or heterotrophic organs and is taken up by sucrose transporters or hexose transporters after cleavage by cell wall-bound invertases (3). Sugars can also be distributed in the subcellular level into different organelles, depending on their actual requirements. During the daytime, many plant species assimilate carbon to synthesize starches, which are transiently stored in chloroplasts. In contrast, sugars remobilize to sink cells or heterotrophic organs during the night (4). In addition, sugars can be imported into the vacuoles for transient or long term storage (5). It is reported that a system for sugar uptake into vacuole is contained in certain plants like sugar beet (6) or maize (7). Under abiotic stress conditions, galactinol and raffinose accumulate in plant cells (8). Overexpression of *GolS2*, which is an abiotic stress-inducible galactinol synthase gene, increases endogenous galactinol and raffinose levels and improves abiotic stress tolerance in *Arabidopsis* (8). These results indicate that sugars might function as osmo-protectants, although little is known about their physiological function under abiotic stresses. The expression of genes not only for sugar synthases but also sugar transporters is induced under abiotic stress conditions (9), and sugars might be transported to specific tissues or organelles under abiotic stress conditions (10).

Physiological analyses showed that both facilitated diffusion and secondary active transporters for sugars exist in plants (11, 12). All of the previously characterized sugar transporters are secondary active transporters (10, 13–15). In many cases, the activities of secondary active transporters in plants are dependent upon proton gradients. STP1 was initially isolated as a plant sugar transporter from *Arabidopsis* and was shown to be a proton/hexose symporter localized at the plasma membrane (13). Sugar transporters for hexose and sucrose uptake across the plasma membrane have been identified in various plant species (16–18). However, little is known about sugar transporters localized at the tonoplast. Recently, two proton-dependent antiporters involved in glucose influx across the tonoplast were identified in *Arabidopsis* (10, 15). On the other hand, the activities of facilitated diffusion transporters depend on substrate concentration and are not dependent upon proton gradients. Because various plant species accumulate a considerable amount of soluble sugars in

* This work was supported by a grant-in-aid for scientific research in priority areas from the Ministry of Education, Culture, Sports, Science, and Technology of Japan.

[S] The on-line version of this article (available at http://www.jbc.org) contains supplemental "Experimental Procedures," Tables S1 and S2, and Figs. S1–S6.

[1] To whom correspondence should be addressed. Tel.: 81-3-5841-8137; Fax: 81-3-5841-8009; E-mail: akys@mail.ecc.u-tokyo.ac.jp.

their vacuoles (5), the existence of facilitated diffusion transporters for the efflux of sugars across the tonoplasts have been predicted for plant cells (11, 19).

ERD6, a member of a multigene family in *Arabidopsis*, has been isolated from a cDNA library prepared from *Arabidopsis* plants exposed to drought stress for 1 h. Sequence analysis of this gene indicated that it encodes a putative sugar transporter (20). Here, we report the characterization of ESL1 (ERD six-like 1), which is a member of the ERD6-like family and an abiotic stress-inducible transporter. We present evidence that ESL1 requires an N-terminal L*XXX*LL motif for its localization to the tonoplast. Furthermore, we analyzed the functional property of ESL1 by using a mutated form of ESL1 that is localized at the plasma membrane in plant cells.

EXPERIMENTAL PROCEDURES

Plant Materials and Growth Conditions—*Arabidopsis thaliana* Columbia ecotype plants were grown on germination medium agar plates with 3% sucrose for 3 weeks under a 16-h light/8-h dark regime as previously described (21). Plants for the transient expression assay were grown on soil under an 8-h light/16-h dark regime. Suspension-cultured tobacco BY-2 cells (*Nicotiana tabacum L.* cv. Bright Yellow 2) were obtained from the Riken Bioresource Center. The cells were subcultured once in Linsmaier and Skoog medium for 5 days at 30 °C in the dark with an orbital shaker. A T-DNA insertional mutant of *ESL1* (SALK_025646) was obtained from the Arabidopsis Biological Resource Center. Information appertaining to the T-DNA insertional mutant was obtained from the website for the Salk Institute Genomic Analysis Laboratory. The T-DNA insertional site was confirmed by PCR using a T-DNA left border primer (LBa1) and an ESL1-specific primer (ESL1-RP) pair. All primer sequences are shown in supplemental Table S2.

RNA Gel Blot Analysis, Quantitative Reverse Transcription-PCR, and Abiotic Stress and Hormone Treatments—Total RNA extraction from 3-week-old *Arabidopsis* plants, RNA gel blot analysis, and qRT-PCR[2] analysis were conducted as previously described (22). For RNA gel blot analysis, each lane was loaded with 7 μg of total RNA, and the full-length cDNA sequence of each gene was used as a probe. For qRT-PCR analysis, cDNA was synthesized from total RNA using SuperScript III (Invitrogen) with random primers according to the manufacturer's instructions. qRT-PCR was performed on a Light Cycler (Roche Applied Science) using SYBR Premix Ex *Taq* kit (Takara) according to the manufacturer's instructions. The *ERD6*, *ESL1* *Atβfruct3*, *Atβfruct4*, and 18 S rRNA fragment were amplified with ERD6-F-qRT and ERD6-R-qRT, ESL1-F-qRT and ESL1-R-qRT, BFRUCT3-F-qRT and BFRUCT3-R-qRT, BFRUCT4-F-qRT and BFRUCT4-R-qRT, and 18S-F-qRT and 18S-R-qRT primer pairs, respectively. For abiotic stress and ABA treatments, the plants were transferred into hydroponic Murashige and Skoog medium at 2 days prior to abiotic stress and hormone treatments. The plants were dehydrated on parafilm or cultured with NaCl and ABA at the concentration of 250 mM and 100 μM, respectively.

Histochemical Localization—The *ERD6* or *ESL1* promoter:*GUS* reporter plasmid was constructed by cloning PCR-amplified fragments containing a 1472- or 1743-bp sequence of the *ERD6* and *ESL1* promoter region, respectively. The following primers were used to amplify DNA fragments for promoter GUS analysis: ERD6pro-EcoRI-F and ERD6pro-XhoI-R for the *ERD6* promoter fragment and ESL1pro-EcoRI-F and ESL1pro-SalI-R for the ESL1 promoter fragment. These fragments were ligated into the pGK-GUS vector (23), and GUS activity was determined as previously described (24). We then constructed the *ERD6* or the *ESL1* promoter:*TM-GFP* construct using the primers ERD6pro-ApaI-F and ERD6pro-XbaI-R for the *ERD6* promoter fragment and ESL1pro-ApaI-F and ESL1pro-SmaI-R for the *ESL1* promoter fragment. These fragments were subsequently ligated into the pGK35S-TM-sGFP vector (supplemental "Experimental Procedures"). GFP fluorescence (excitation filter, 488 nm; emission filter bandpass, 505- 530 nm) was observed with a laser scanning confocal microscope (LSM510; Zeiss).

Subcellular Localization of ESL1—Transient expression assay using mesophyll protoplasts from *Arabidopsis* were performed as previously described (25). For cloning of the 35Spro:*ESL1-GFP* construct, the fragment of the *ESL1* coding region was amplified by PCR from *Arabidopsis* cDNA with the ESL1-BamHI-F and ESL1-BamHI-R primer pair. The *ESL1* fragment was ligated into the BamHI site of the pGK35S-sGFP vector (supplemental "Experimental Procedures"). We established stable BY-2 cell lines expressing GFP-fused ESL1 or ESL1(LLL/AAA) to analyze their respective subcellular localization. BY-2 cells were transformed with each plasmid via *Agrobacterium tumefaciens* (strain EHA105) according to the previously established method (26). The *ESL1* fragment was amplified by PCR with the ESL1-BamHI-F and ESL1-BamHI-R primer pair and was ligated into the pBE2113-CsGFP vector (supplemental "Experimental Procedures"). To generate an ESL1(LLL/AAA) fragment, we used the ESL1(LLL/AAA)-BamHI-F and ESL1-BamHI-R primer pair. For alanine scanning analysis, we used the forward primers, ESL1(L10A)-BamHI-F, ESL1(E11A)-BamHI-F, ESL1(G13A)-BamHI-F, ESL1(L14A)-BamHI-F, ESL1(L15A)-BamHI-F, and ESL1(L16A)-BamHI-F. We used ESL1-BamHI-R as the reverse primer for the amplification of the fragments utilized for the alanine scanning assay. For the co-localization assay, we amplified the *ESL1* fragment with the ESL1-XbaI-F and ESL1-SmaI-R primer pair, and the fragment was subsequently ligated into the pGKX-cYFP vector (supplemental "Experimental Procedures"). We then constructed the CFP-VAM3 construct using the primers VAM3-NotI-F and VAM3-XhoI-R to amplify *VAM3* from *Arabidopsis* cDNA. The *VAM3* fragment was subsequently ligated into the pBI22135S-nCFP vector (supplemental "Experimental Procedures"). GFP fluorescence, YFP fluorescence (excitation filter, 514 nm; emission filter bandpass, 530/30 nm), CFP fluorescence (excitation filter, 458 nm; emission filter bandpass, 482.5/30 nm), and chlorophyll autofluorescence (exci-

[2] The abbreviations used are: qRT, quantitative reverse transcription; GFP, green fluorescent protein; MES, 4-morpholineethanesulfonic acid; CCCP, carbonyl cyanide *m*-chlorophenylhydrazone; Wm, wortmannin; BFA, brefeldin A; ABA, abscisic acid; GUS, β-glucuronidase.

tation filter, 543 nm; emission filter bandpass, ≥560 nm) were observed with the laser scanning confocal microscope.

Functional Characterization of ESL1—To measure glucose transport activity by using suspension-cultured tobacco BY-2 cells, we established transgenic BY-2 cell lines expressing ESL1 or ESL1(LLL/AAA). The *ESL1* fragment was amplified by PCR with the primers ESL1-BamHI-F and ESL1-BamHI-R2 for the 35Spro:*ESL1* construct, and the *ESL1(LLL/AAA)* fragment was amplified with the ESL1(LLL/AAA)-BamHI-F and ESL1-BamHI-R2 primers for the 35Spro:*ESL1(LLL/AAA)* construct. Each fragment was ligated into the pBE2113Not vector, and transport activity was subsequently measured by a previously described method with modifications (27). Briefly, the accumulation of glucose was measured in 0.5-ml aliquots of cell suspension. First, each suspension was filtered. After filtering, the suspensions were resuspended in uptake buffer (20 mM MES, 0.5 mM $CaSO_4$; pH adjusted to 5.7 with KOH) and equilibrated for 45 min with continuous orbital shaking. Equilibrated cells were collected by filtration and resuspended in fresh uptake buffer to obtain a density of 200 mg of cells/ml. The cells were incubated on the orbital shaker for 1.5 h in darkness at 30 °C. To start the reaction, 450 μl of cells were mixed with 50 μl of medium containing 3.7 or 7.4 kBq [U-^{14}C]glucose (CFB96; GE Healthcare). The total glucose concentration was adjusted by adding unlabeled glucose. After incubation at 30 °C for 10 min, the reaction was stopped by dilution with 10 ml of ice-cold washing buffer (20 mM MES, 0.5 mM $CaSO_4$; pH adjusted to 6.5 with KOH). The cells were collected on a 25-mm glass fiber filter (GF/B; Whatman) and rinsed by the further addition of 5 ml of washing buffer. The filters were dissolved in a scintillation mixture (Clear-sol; Nacalai Tesque), and their radioactivities were counted (LS6000; Beckman). The competitors or the inhibitor were added 30 s prior to the addition of [^{14}C]glucose.

Invertase Assay—All of the steps were performed at 4 °C unless otherwise noted. The measurement of acid invertase activity was performed as previously described (28, 29) with minor modifications. Three-week-old *Arabidopsis* plants were homogenized in an extraction buffer (20 mM sodium phosphate, 1 mM EDTA, 1 mM EGTA, 1 mM $MgCl_2$, 1 mM $MnCl_2$, 5 mM dithiothreitol, pH 6.5) and centrifuged (10 min at 27,000 × *g*). The supernatant was desalted on a gel filtration column (PD10; GE Healthcare) and was used as the source of the soluble invertase. The pellet from centrifugation of a homogenate was washed twice with the extraction buffer. The cell wall-bound acid invertase was solubilized from the wash pellet with the extraction buffer containing 1 M NaCl by shaking for 5 h. The resultant soluble fraction was used for the assay without desalting and was used as the source of the insoluble invertase. For the acid invertase activity assay, we used a solution containing 40 μl of 0.4 M sodium acetate (pH 5.0), 10 μl of 1 M sucrose, and 50 μl of extraction enzyme (soluble enzyme, 20 μg; insoluble enzyme, 5 μg) in a final volume of 100 μl. Incubation was carried out at 37 °C for 30 min. The reaction was stopped at 95 °C for 5 min, and the reaction solution was neutralized by the addition of 10 μl of 1 M KOH. The concentration of glucose was determined with an F-kit (Roche Applied Science).

RESULTS

Comparative Analysis of Amino Acid Sequences of the ERD6-like Transporters—Supplemental Fig. S1*A* presents a phylogenic tree based on the amino acid sequences of 53 *Arabidopsis* proteins exhibiting homology to the monosaccharide transporter STP1 (13), 10 human glucose transporters (GLUT), and a *myo*-inositol transporter (HMIT). Seven families of monosaccharide transporters exist in *Arabidopsis* including the 19-member ERD6-like family as the largest monosaccharide transporter family in *Arabidopsis*. *ERD6* was isolated from an *Arabidopsis* cDNA library from plants that were exposed to drought stress for 1 h (20). A cDNA of a homologous ERD6-like family gene was isolated from sugar beet (*Beta vulgaris*) by PCR-based cloning (30). In addition, we found ERD6-like family homologous genes in various plant species from GenBank™ in dicots such as barrel medic (*Medicago truncatula*; GenBank™ accession number ABN08184) and Grape vine (*Vitis vinifera*; CAO22837), in monocots such as rice (*Oryza sativa*; BAF12080) and corn (*Zea mays*; ACG32874), in gymnosperms such as Sitka spruce (*Picea sitchensis*; ABK25410), and in moss such as *Physcomitrella patens* (XP_001782547).

The ERD6-like family shows low homology to any previously characterized *Arabidopsis* monosaccharide transporters. However, they exhibited high homology to mammalian glucose transporters, especially GLUT6 and GLUT8 (supplemental Fig. S1*A*). From a phylogenic analysis of the ERD6-like family in *Arabidopsis*, we identified a close homologue of ERD6, which we named ESL1 (ERD six-like 1) (supplemental Fig. S1*B*). Analysis of ERD6 and ESL1 revealed 12 putative transmembrane domains and conserved sequences among the major facilitated superfamily (supplemental Fig. S1*C*), as well as all previously characterized monosaccharide transporters. An *N*-glycosylation site in loop 9, a feature shared between GLUT6 and GLUT8 (31), was not found in ERD6 and ESL1.

Expression Analyses—To examine the physiological functions of ERD6 and those of ESL1 under abiotic stresses, we initially analyzed their expression patterns under abiotic stress conditions and ABA treatment with RNA gel blot hybridization (Fig. 1*A*). In good accordance to a previous study (32), maximal accumulation of *ERD6* mRNA was detected after 1 and 2 h of exposure to drought stress. The expression of *ESL1* was induced within 1 h and was strongly expressed after 5 h under abiotic stresses. ABA treatment had a converse effect on the expression patterns of *ERD6* and *ESL1*. Accumulation of the *ESL1* mRNA was increased after 5 h in ABA treatment, whereas that of *ERD6* was decreased. We next investigated the changes of the expression in leaves and roots under high salinity and ABA treatment by qRT-PCR analysis (Fig. 1*B*). The expression level of *ERD6* was similar in both leaves and roots under normal conditions. However, its expression in leaves was decreased after exposure to the high salinity and ABA treatment, whereas root expression levels were not reduced. On the other hand, *ESL1* expression was higher in roots than in leaves under normal conditions. The mRNA accumulation of *ESL1* in roots under the high salinity and ABA treatment was also higher than that in leaves. These results were in good accordance with the

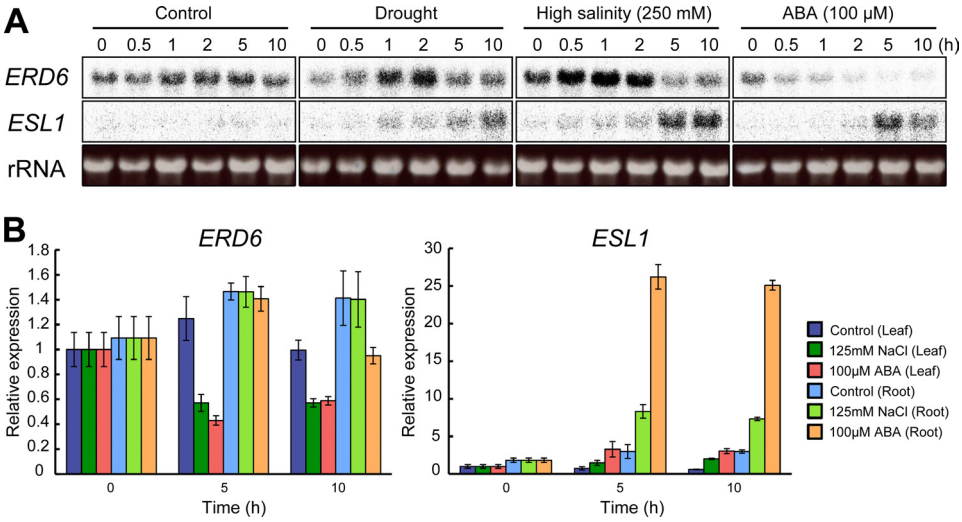

FIGURE 1. **Expression analysis of *ERD6* and *ESL1* under abiotic stress conditions and ABA treatment.** Total RNA from whole plants, leaves, and roots were used for Northern blot (*A*) and qRT-PCR analyses (*B*), respectively. The value of control (leaf) was set to 1.0. To normalize *ERD6* and *ESL1* expression, 18 S rRNA was amplified as an internal control.

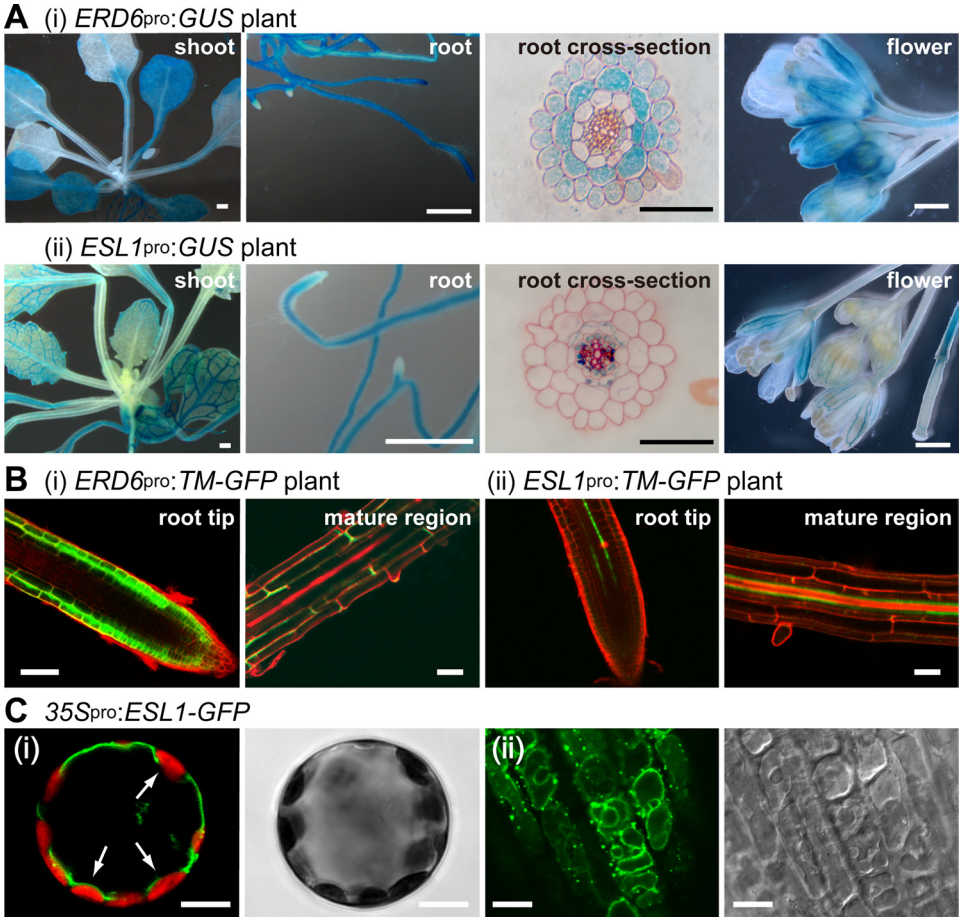

FIGURE 2. **Histological expression profiles and subcellular localization.** *A*, *panel i*, *ERD6*pro:*GUS* plant. *Panel ii*, *ESL1*pro:*GUS* plant. *White bars*, 1 mm; *black bars*, 100 μm. *B*, *panel i*, *ERD6*pro:*TM-GFP* plant. *Panel ii*, *ERD6*pro:*TM-GFP* plant. *Red* indicates propidium iodide staining of cell walls. *Bars*, 50 μm. *C*, *panel i*, transient expression of ESL1-GFP fusion protein in *Arabidopsis* protoplasts. The *left panel* shows a merged image of GFP fluorescence and chloroplast autofluorescence. The *right panel* is the image obtained by Nomarski differential interference contrast microscopy. The *arrows* indicate that GFP fluorescence separated its volume from cytoplasm containing chloroplasts. *Bars*, 10 μm. *Panel ii*, subcellular localization of ESL1-GFP fusion proteins in epidermal cells of roots in 35Spro:*ESL1-GFP* transgenic plants. The *left panel* shows the image of GFP fluorescence, and the *right panel* is the image obtained from Nomarski differential interference contrast microscopy. *Bar*, 10 μm.

data from the public microarray data base (supplemental Fig. S2*A*).

Histological Expression Profiles—To determine the histological expression profiles of *ERD6* and *ESL1*, we first generated *ERD6*pro:*GUS* and *ESL1*pro:*GUS* transgenic plants. *GUS* expression was detected in both shoots and roots of the *ERD6*pro:*GUS* and *ESL1*pro:*GUS* plants (Fig. 2*A*). In flowers, GUS staining was detected in sepals of the *ERD6*pro:*GUS* and *ESL1*pro:*GUS* plants (Fig. 2*A*). Furthermore, in *ERD6*pro:*GUS* plants, GUS staining was observed in epidermal and cortex cells of roots and was especially strong in cortex cells (Fig. 2*A*, *panel i*). On the other hand, in *ESL1*pro:*GUS* plants, GUS staining was strongly detected in pericycle and xylem parenchyma cells of roots and also detected in the root endodermis (Fig. 2*A*, *panel ii*). As our next approach, we generated *ERD6*pro:*TM-GFP* and *ESL1*pro:*TM-GFP* transgenic plants. TM-GFP is a membrane-localized GFP fused to the N-terminal half of the monosaccharide transporter, STP9 (33). Although free GFP diffuses through plasmodesmata, TM-GFP does not diffuse for being localized at membrane. In the root tips and the mature region of roots, GFP fluorescence was mainly detected in epidermal and cortex cells of the *ERD6*pro:*TM-GFP* plants (Fig. 2*B*, *panel i*), and it was strongly detected in pericycle and xylem parenchyma cells of the *ESL1*pro:*TM-GFP* plants (Fig. 2*B*, *panel ii*). The results of the promoter:*TM-GFP* plants were coincident with those of promoter:*GUS* plants.

ERD6 and ESL1 showed differences in expression patterns and histological localizations. These results suggest that ERD6 and ESL1 may have different physiological functions. A number of abiotic stress-inducible genes have been identified in various plant species, and the products of these genes function in abiotic stress responses and tolerance (34). The induction pattern of *ESL1* gene expression under abiotic stress conditions was similar to

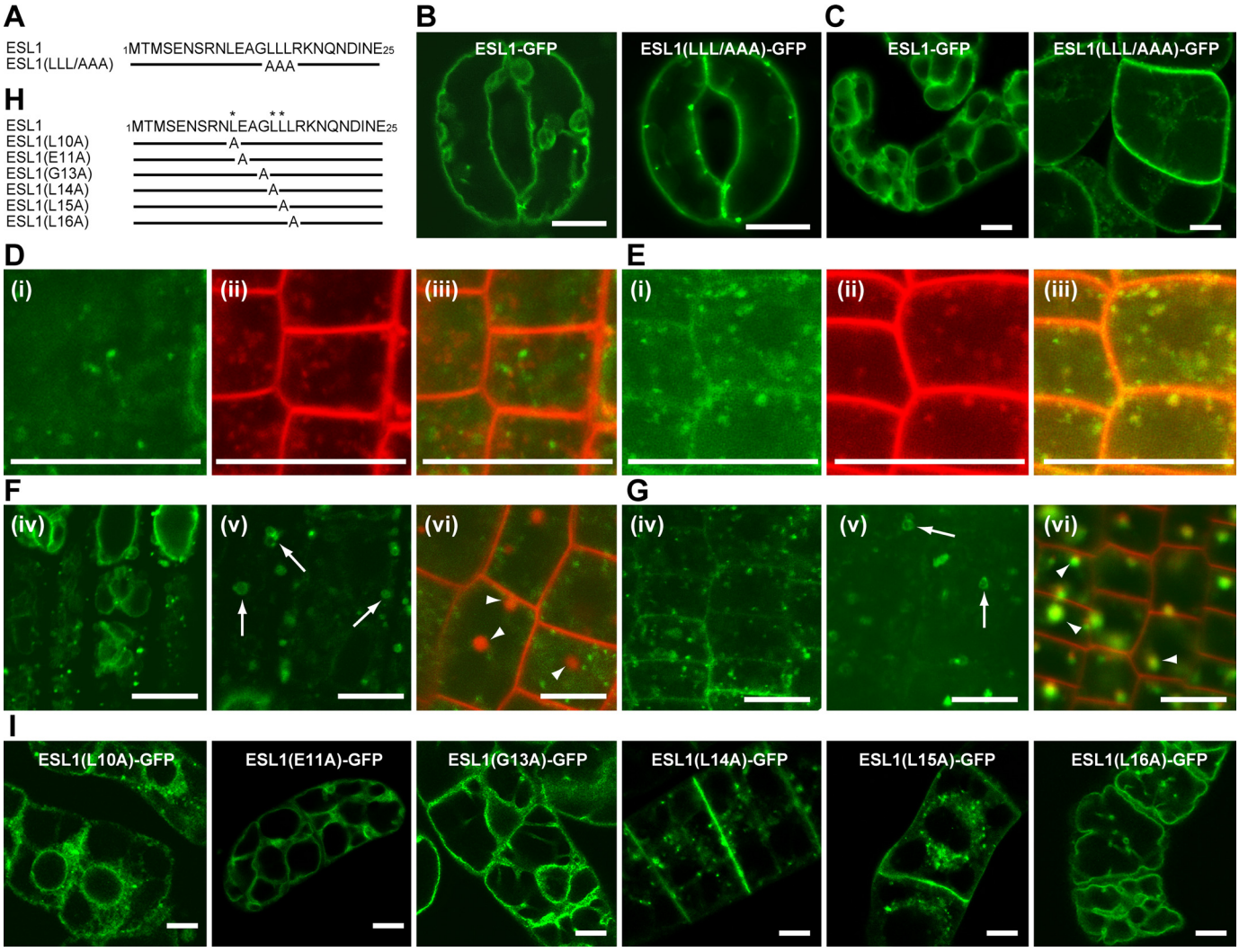

FIGURE 3. **The di-leucine-based sorting signal in the N terminus of ESL1.** *A*, the N-terminal sequence between ESL1 and ESL1(LLL/AAA). *B* and *C*, the subcellular localization of the ESL1-GFP and ESL1(LLL/AAA)-GFP fusion proteins in guard cells of transgenic *Arabidopsis* plants (*B*) and transgenic tobacco BY-2 suspension cells (*C*). *D* and *E*, co-localization assay with FM4-64. Subcellular localization of ESL1-GFP (*D*) and ESL1(LLL/AAA)-GFP (*E*) fusion proteins in *Arabidopsis* transgenic plants is shown. Roots of 5-day-old seedlings expressed ESL1-GFP or ESL1(LLL/AAA)-GFP after 5 μM FM4-64 treatment. Fluorescence of GFP and FM4-64 is indicated in *panels i* and *ii*, respectively. Co-staining with FM4-64 is shown in *panel iii*. *F* and *G*, sensitivity to membrane traffic inhibitors, wortmannin (*panel v*) and BFA (*panel vi*). Roots of 5-day-old seedlings expressed ESL1-GFP (*F*) or ESL1(LLL/AAA)-GFP (*G*) after 60 min of 33.3 μM Wm treatment or after 60 min of 50 μM BFA and 5 μM FM4-64 treatment. *Red* indicates vesicles that were dyed by FM4-64. The *arrows* indicate Wm compartments, and the *arrowheads* indicate BFA compartments. *H* and *I*, alanine-scanning mutagenesis analysis of the N-terminal region of ESL1. *Asterisks* indicate the essential leucine residues necessary for ESL1-GFP to localize to the tonoplast. *Bars*, 10 μm.

those of abiotic stress-inducible genes. Therefore, we focused our functional characterization on ESL1 in this study.

ESL1 Localization at the Tonoplast Requires an N-terminal Di-leucine-like Motif—The subcellular localization of ESL1 was studied in *Arabidopsis* mesophyll protoplasts that transiently expressed a GFP-fused ESL1 protein (ESL1-GFP) driven by the 35S promoter, revealing the localization at the tonoplast (Fig. 2*C*, *panel i*). Co-localization of signals at the tonoplast was also observed when expressed with the CFP-VAM3 tonoplast marker (supplemental Fig. S3). We next established transgenic *Arabidopsis* plants expressing ESL1-GFP (35Spro:*ESL1-GFP*). In the 35Spro:*ESL1-GFP* plants, GFP fluorescence was observed at tonoplasts and vesicular structures (Fig. 2*C*, *panel ii*). GLUT8, which is a mammalian homologue of the ERD6-like family, is localized at the late endosome or the lysosome (35). GLUT8 contains an N-terminal acidic di-leucine motif E*XXX*L(L/I). When this motif was mutated, GLUT8 was mislocalized to the plasma membrane (36). Interestingly, we noted that most of the transporters in the ERD6-like family also contain a di-leucine or a tri-leucine sequence in their N termini (supplemental Fig. S4*A*). For the case of ESL1, it contained a tri-leucine sequence in its N terminus.

Stemming from the observations gained from mammalian studies, we hypothesized that di-leucine or tri-leucine sequences in the N termini of ERD6-like transporters also determine their subcellular localizations. As a result, we generated ESL1(LLL/AAA)-GFP, in which the tri-leucine of ESL1 was mutated into a tri-alanine (Fig. 3*A*). Fluorescence of ESL1(LLL/AAA)-GFP was localized to many vesicular structures and the plasma membrane and not at the tonoplast in *Arabidopsis* plants and tobacco BY-2 suspension cells (Fig. 3, *B* and *C*).

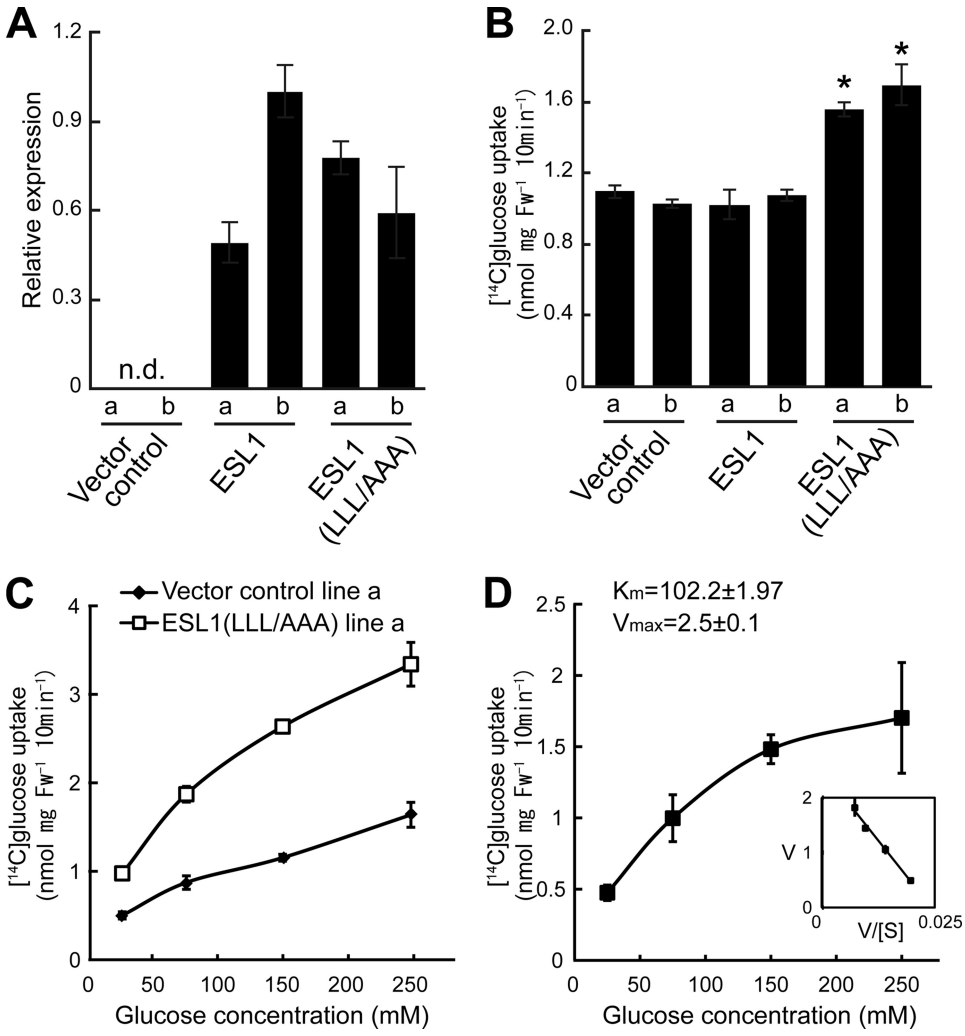

FIGURE 4. **Kinetics analysis of glucose uptake activity of ESL1(LLL/AAA).** *A*, relative expression of ESL1 in transgenic BY-2 cells determined by qRT-PCR. The highest expression level was set to 1.0. To normalize *ESL1* expression, 18 S rRNA was amplified as an internal control. The data represent the means and the standard error of three replications. *n.d.*, not detected. *B*, glucose (50 mM) uptake activity of tonoplast-localized ESL1 and that of plasma membrane-localized ESL1(LLL/AAA) in BY-2 cells. In relative comparison with the vector control line a, statistical significance at a level of $p < 0.01$ is indicated by an *asterisk*. *C*, concentration-dependent glucose uptake activity of ESL1(LLL/AAA) and that of the vector control line a in BY-2 cells. *D*, net activity of ESL1(LLL/AAA). The presented values represent the subtraction of glucose uptake activity of vector control cells from that of ERD6(LLL/AAA)-expressing cells in *C*. Uptake data were fitted to Michaelis-Menten and Eadie-Hoftee (*inset*) equations. Each value represents the mean ± S.D. ($n \geq 3$). *Fw*, fresh weight.

The lipophilic styryl dye (FM4-64) is known as an endocytic marker (37). This dye is transferred from the plasma membrane via endosomes to the vacuole when exogenously added to plant cells. We tried to use this dye as a means to analyze the localizations of ESL1 and ESL1(LLL/AAA). Fifteen min after the addition of FM4-64, ESL1-GFP showed only weak co-localization with the FM4-64 positive endosomes in *Arabidopsis* root cells (Fig. 3*D*, *panel iii*). In contrast, the majority of ESL1(LLL/AAA)-GFP signals were co-stained with FM4-64 (Fig. 3*E*, *panel iii*). Furthermore, we analyzed the effects of vesicle trafficking inhibitors, wortmannin (Wm) and brefeldin A (BFA). Wm is an inhibitor of phosphatidylinositol-3-OH kinase, and BFA is a fungal toxin that inhibits the guanine-nucleotide exchange factor. In *Arabidopsis* root cells, Wm leads to the vacuolation (Wm compartment) of endosomes, such as the prevacuolar compartment or multivesicular body (38). BFA causes the *trans*-Golgi network or early endosome to aggregate with the FM4-64, and they are located inside an aberrant compartment (BFA compartment) (38). Under Wm treatment, we detected Wm compartments in both 35Spro:*ESL1-GFP* and 35Spro:*ESL1(LLL/AAA)-GFP* plants (Fig. 3, *F*, *panel v*, and *G*, *panel v*). However, we detected BFA compartments in only 35Spro:*ESL1(LLL/AAA)-GFP* plants under BFA treatment (Fig. 3, *F*, *panel vi*, and *G*, *panel vi*). These results indicate that ESL1 and ESL1(LLL/AAA) are localized at different intracellular compartments. Thus, the N-terminal tri-leucine sequence of ESL1 plays a functional role for its subcellular sorting signal.

We next performed alanine-scanning mutagenesis in the N-terminal region containing the tri-leucine sequence to identify the critical residues for the tonoplast localization of ESL1 (Fig. 3*I*). In transgenic BY-2 cells, ESL1(L10A)-GFP appeared to be localized mainly at the endoplasmic reticulum, whereas ESL1(L14A)-GFP and ESL1(L15A)-GFP were localized to the plasma membrane (Fig. 3*I*). Thus, the L*XXX*LL motif was essential for ESL1 to be sorted to the tonoplast in plant cells.

ESL1 Was a Facilitated Diffusion Transporter for Monosaccharide—To verify whether ESL1 is a functional monosaccharide transporter, we generated transgenic BY-2 cells expressing *ESL1* (Fig. 4*A*). However, a similar level of glucose was observed in ESL1-expressing cells and vector control cells (Fig. 4*B*). We suspected that the lack of transporter activity was due to the tonoplast localization of ESL1. Therefore, we subsequently established transgenic BY-2 cells expressing plasma membrane localized *ESL1(LLL/AAA)* (Fig. 4*A*). In contrast to the aforementioned results, these cells exhibited significantly higher glucose uptake activity relative to vector control cells (Fig. 4*B*). We then analyzed the kinetics of glucose transport activity of ESL1(LLL/AAA) using the substrate concentration between 25 and 250 mM (Fig. 4*C*). Because BY-2 cells exhibited a naturally high background of glucose uptake ability (Fig. 4*C*), we calculated the net activities of ESL1(LLL/AAA), which were determined by the subtracted values of glucose uptake of vector control cells from those of ESL1(LLL/AAA)-expressing cells (Fig. 4*D*). K_m and V_{max} values of ESL1(LLL/AAA) for glucose were 102.2 ± 2.0 mM and 2.5 ± 0.1 nmol mg fresh weight^{-1} 10 min^{-1}, respectively.

TABLE 1

Inhibition of [^{14}C]glucose uptake by various compounds in the ESL1(LLL/AAA) line a

The [^{14}C]glucose concentration was 5 mM when competing carbohydrates were added and 50 mM when CCCP was added.

Added compound	Uptake
	% of control
Control (no competitor or inhibitor)	100.0
125 mM D-glucose	22.2 ± 1.4
125 mM L-glucose	95.7 ± 2.1
125 mM 2-deoxy-D-glucose	27.4 ± 2.9
125 mM D-fructose	65.5 ± 1.8
125 mM D-galactose	45.1 ± 3.5
125 mM D-mannose	54.7 ± 2.7
125 mM D-xylose	76.5 ± 3.2
125 mM D-sorbitol	102.8 ± 7.5
125 mM D-mannitol	111.9 ± 2.6
125 mM *myo*-inositol	111.7 ± 3.6
125 mM D-glucosamine hydrochloride	109.2 ± 7.1
125 mM sucrose	109.7 ± 4.3
125 mM maltose	117.4 ± 2.8
100 μM CCCP	104.9 ± 2.8

Table 1 shows the sensitivities of ESL1(LLL/AAA)-dependent transport to competitors or an inhibitor. The uptake of [^{14}C]glucose was significantly inhibited by hexoses such as glucose, fructose, galactose, and mannose and a pentose (xylose), with glucose showing the highest level of inhibition. The addition of linear or circular polyols, glucosamine, and disaccharides did not affect the [^{14}C]glucose uptake activity of ESL1(LLL/AAA). Furthermore, reduction of the proton gradient caused by the protonophore (CCCP) did not have any effect on the transport activity of ESL1(LLL/AAA) cells, although glucose uptake activity of vector control cells was inhibited by adding CCCP (supplemental Table S1). These data suggest that ESL1 functions as a low affinity facilitated diffusion transporter for monosaccharides.

Vacuolar Invertase Activity Is Increased under Abiotic Stress Conditions—To determine the physiological role of ESL1 in plant cells, it is important to have an understanding regarding the amount of hexose in vacuoles. Invertases are considered as key enzymes to convert sucrose into glucose and fructose. Degradation of sucrose by vacuolar invertase is one of the sources for vacuolar hexose (39). We then analyzed vacuolar invertase activity under abiotic stress conditions. We measured the vacuolar and cell wall-bound invertase activity when *Arabidopsis* plants were exposed to abiotic stresses or ABA treatment for 5 h. Vacuolar invertase activity for soluble acid invertases was increased under abiotic stress conditions and ABA treatment (supplemental Fig. S5*A*). Particularly, vacuolar invertase activity under drought and ABA treatments was higher than that under high salinity conditions. Cell wall-bound invertase activity for insoluble acid invertases did not change (supplemental Fig. S5*B*). These results suggest that hexoses were accumulated in the vacuole under exposure to abiotic stress conditions.

There are two vacuolar invertase genes (*Atβfruct3* and *Atβfruct4*) in *Arabidopsis* (40). We analyzed the expression patterns of those genes under abiotic stress conditions (supplemental Fig. S5*C*). The transcript level of *Atβfruct3* increased after exposure to 2 h of drought and ABA treatments and exposure to 5 h of high salinity. At the 5-h time point, the mRNA accumulation of *Atβfruct3* under drought and ABA treatment was also higher than that under the high salinity condition. These results showed positive correlation between mRNA accumulation and the activity of vacuolar invertases. Moreover, we investigated the expression of the vacuolar invertase genes in leaves and roots (supplemental Fig. S5*D*). The expression of *Atβfruct3* was mainly detected in roots. The mRNA induction pattern of *Atβfruct3* in leaves and roots was similar to that of *ESL1* under high salinity and ABA treatment (Fig. 1*B*). On the other hand, the expression of *Atβfruct4* was mainly detected in leaves. According to data from the public microarray data base, the histological expression patterns of the vacuolar invertase genes were partially overlapped with that of *ESL1* (supplemental Fig. S2*B*). ESL1 might coordinately function with the vacuolar invertases in those cells in which both *ESL1* and the vacuolar invertase genes are expressed.

Analysis of a T-DNA Insertional Mutant of ESL1 under High Salinity Conditions—We identified a mutant line (SALK_025646) carrying a T-DNA insertion in the fifth exon of the ESL1 gene (supplemental Fig. S6*A*). The T-DNA insertional mutant, which we designated as *esl1-1*, was a knock-out mutant because the *ESL1* mRNA was not accumulated in *esl1-1* (supplemental Fig. S6*B*). We observed no differences between the root lengths of this mutant and those of wild-type plants under high salinity conditions (supplemental Fig. S6*C*). The ERD6-like family is the largest monosaccharide transporter family in *Arabidopsis* containing 19 genes. It is possible that additional genes in the ERD6-like family may function redundantly with ESL1.

DISCUSSION

In this study, we characterized the abiotic stress-inducible monosaccharide transporter ESL1, which belongs to the ERD6-like gene family. The analysis of glucose uptake activity using transgenic tobacco BY-2 suspension cells revealed that ESL1(LLL/AAA), which is localized at the plasma membrane, functions as a low affinity transporter for monosaccharides. Its K_m value was exceptionally high and showed lower affinity to glucose (Fig. 4*D*) compared with previously characterized sugar transporters such as STP1 (about 20 μM) (13), PLT5 (about 2 mM) (14, 41), or VGT1 (about 4 mM) (15). Moreover, the transport activity of ESL1(LLL/AAA) was not affected by the reduction of the proton gradient caused by a protonophore (Table 1), thereby indicating that ESL1 is a facilitated diffusion transporter. Although physiological features on plasma membrane might be different from those on the tonoplast, it is difficult to assay the functions of transporters that are localized at the tonoplast in appropriate systems using plant cells. In this study, we measured the activity of the mutated ESL1, ESL1(LLL/AAA), in plant cells. All previously characterized monosaccharide transporters in *Arabidopsis* are secondary active transport systems that are dependent on a proton gradient. To date, facilitated diffusion transporters for sugars have not been isolated, although biochemical experiments indicated that sugar-specific facilitated diffusion transporters exist in plant cells (11, 12).

Using the GFP reporter gene in both protoplasts and transgenic *Arabidopsis* plants, we showed that the ESL1 protein is mainly localized at tonoplasts (Figs. 2*C* and 3*B*). Because the K_m value of ESL1(LLL/AAA) in BY-2 cells was approximately

100 mM, hexoses should accumulate to a concentration of nearly 100 mM in the vacuole under abiotic stress conditions to obtain sufficient activity. Degradation from sucrose by invertases is one of the sources for hexose in the vacuole (39). In maize, expression of a vacuolar invertase gene is increased by drought stress and ABA treatment (42, 43). We showed that vacuolar invertase activity in *Arabidopsis* was also increased by drought, high salt stress, and ABA treatment (supplemental Fig. S5*A*). Hexose levels in the vacuole might be increased by vacuolar invertase under abiotic stresses. Because the expression patterns of the vacuolar invertase genes were similar to that of *ESL1* (supplemental Figs. S2*B* and S5*D*), ESL1 might work coordinately with the vacuolar invertase to accumulate hexoses in plant cells under abiotic stress conditions.

Sugars (*e.g.* glucose, sucrose, galactinol, and raffinose) accumulate in plant cells under abiotic stress conditions (8). In addition, it is thought that the vacuole functions as a storage organelle for soluble sugars. Some previous reports indicated that hexoses in the vacuole account for more than 90% of the total hexose content in various plant species (5). Because the direction of transport for facilitated diffusion transporters depends upon a substrate concentration gradient, ESL1 may function in the efflux of hexoses from the vacuole to the cytoplasm as a mechanism to regulate sugar remobilization and osmotic pressure under abiotic stress conditions.

It is reported that the change of subcellular localization of a mammalian glucose transporter by endocytic trafficking regulates its transport activity (44). For example, GLUT4 is deposited at intracellular compartments during its unstimulated state and is acutely redistributed to the plasma membrane for the uptake of glucose in response to insulin and other stimuli (44). The C-terminal di-leucine motif in GLUT4 has been shown to be functionally involved in this dynamic intracellular distribution response. We then tested whether the intracellular trafficking of ESL1 was also regulated by stimuli. However, we could not observe any changes in the localization of ESL1 under our experimental conditions using *Arabidopsis* mesophyll protoplasts (data not shown).

The alanine scanning analysis of the N-terminal region of ESL1 determined that an L*XXX*LL motif was essential to its localization at the tonoplast (Fig. 3*I*). Moreover, ESL2 also contains this motif in its N terminus (supplemental Fig. S4*A*) and was also localized at the tonoplast (supplemental Fig. S4*B*). Collectively, these results indicated that the L*XXX*LL motif potentially functions as a sorting signal of ERD6-like transporters to the tonoplast. There are many reports for two types of di-leucine motifs from mammals and yeast: the acidic di-leucine motif E*XXX*(L/I) and the acidic cluster di-leucine motif D*XX*LL (45). We found that an acidic di-leucine motif (LEAGLL) overlaps the L*XXX*LL motif sequence in the N terminus of ESL1. However amino acid substitution in this acidic di-leucine motif did not affect the subcellular localization of ESL1 in BY-2 cells (Fig. 3*I*). Therefore, the L*XXX*LL motif appears to be a novel di-leucine motif that functions as a sorting signal in plants. We found the L*XXX*LL motif in the N termini of ERD6-like transporters in various plants other than *Arabidopsis*, even in gymnosperms such as Sitka spruce (*P. sitchensis*; ABK24356) and in moss such as *P. patens* (XP_001782547). Interestingly, this motif was not found in the N termini of non-plant ERD6-like transporters, such as human GLUT8, red imported fire ant (*Solenopsis invicta*; AAX92638), and starlet sea anemone (*Nematostella vectensis;* XP_001634924).

A common feature between the L*XXX*LL motif and reported di-leucine motifs from mammals and yeast is that two leucine residues are conserved in-line. The two leucine residues are known to be essential for interaction with adaptor proteins related with membrane traffic. For example, Nef, which is an accessory protein of the human immunodeficiency virus, has the ability to redistribute CD4 from the plasma membrane to the interacellular compartment by the interaction between its acidic di-leucine motif and adaptor proteins. Mutations of leucine residues of its acidic di-leucine motif abolished the ability of Nef, whereas mutations of other neighboring residues of the leucine had no effect (46). In the case of ESL1, each mutation of two leucine residues of L*XXX*LL, ESL1(L14A) and ESL1(L15A), changed the localization of ESL1 from the tonoplast to the plasma membrane (Fig. 3*I*), indicating that function of the L*XXX*LL motif was disrupted by the mutations. On the other hand, ESL1(L10A) appeared to be localized mainly at the endoplasmic reticulum (Fig. 3*I*). We considered that the A*XXX*LL sequence might change the affinity for binding to the adaptor proteins or have the ability to interact with other adaptor proteins. Future analysis of the adaptor proteins that interact with the L*XXX*LL motif would provide more information pertaining to the mechanisms of membrane trafficking in plants.

In conclusion, we isolated ESL1 as an abiotic stress-inducible gene and functionally characterized ESL1 as the facilitated diffusion transporter for monosaccharides from plants using mutated ESL1. ESL1 was localized at the tonoplast, and its N-terminal L*XXX*LL motif was essential for proper subcellular sorting to the tonoplast. Moreover, we confirmed that the activity of vacuolar invertase was increased during abiotic stress conditions, and the expression patterns of the vacuolar invertase genes were similar to that of *ESL1*. Therefore, we hypothesize that ESL1 regulates sugar remobilization and cellular osmotic pressure in a coordinated response with the vacuolar invertase in plant cells under abiotic stresses.

Acknowledgments—We thank Dr. Michihiro Kasahara (Teikyo University, Tokyo, Japan) and Dr. Maki Katsuhara (Okayama University, Okayama, Japan) for technical advice and discussion. We also thank Kyoko Yoshiwara and Dr. Yusuke Ito (Japan International Research Center for Agricultural Sciences, Ibaraki, Japan) for technical support and Dr. Yasuo Niwa (Shizuoka Prefectural University, Shizuoka, Japan) for providing us with the sGFP gene.

REFERENCES

1. Williams, L. E., Lemoine, R., and Sauer, N. (2000) *Trends Plant Sci.* **5,** 283–290
2. Lalonde, S., Wipf, D., and Frommer, W. B. (2004) *Annu. Rev. Plant Biol.* **55,** 341–372
3. Rolland, F., Baena-Gonzalez, E., and Sheen, J. (2006) *Annu. Rev. Plant Biol.* **57,** 675–709
4. Smith, A. M., Zeeman, S. C., and Smith, S. M. (2005) *Annu. Rev. Plant Biol.* **56,** 73–98
5. Voitsekhovskaja, O. V., Koroleva, O. A., Batashev, D. R., Knop, C., Tomos,

A. D., Gamalei, Y. V., Heldt, H. W., and Lohaus, G. (2006) *Plant Physiol.* **140,** 383–395
6. Briskin, D. P., Thornley, W. R., and Wyse, R. E. (1985) *Plant Physiol.* **78,** 871–875
7. Rausch, T., Butcher, D. N., and Taiz, L. (1987) *Plant Physiol.* **85,** 996–999
8. Taji, T., Ohsumi, C., Iuchi, S., Seki, M., Kasuga, M., Kobayashi, M., Yamaguchi-Shinozaki, K., and Shinozaki, K. (2002) *Plant J.* **29,** 417–426
9. Maruyama, K., Sakuma, Y., Kasuga, M., Ito, Y., Seki, M., Goda, H., Shimada, Y., Yoshida, S., Shinozaki, K., and Yamaguchi-Shinozaki, K. (2004) *Plant J.* **38,** 982–993
10. Wormit, A., Trentmann, O., Feifer, I., Lohr, C., Tjaden, J., Meyer, S., Schmidt, U., Martinoia, E., and Neuhaus, H. E. (2006) *Plant Cell* **18,** 3476–3490
11. Martinoia, E., Kaiser, G., Schramm, M. J., and Heber, U. (1987) *J. Plant Physiol.* **131,** 467–478
12. Sacchi, G. A., Abruzzese, A., Lucchini, G., Fiorani, F., and Cocucci, S. (2000) *Plant Soil* **220,** 1–11
13. Sauer, N., Friedländer, K., and Gräml-Wicke, U. (1990) *EMBO J.* **9,** 3045–3050
14. Klepek, Y. S., Geiger, D., Stadler, R., Klebl, F., Landouar-Arsivaud, L., Lemoine, R., Hedrich, R., and Sauer, N. (2005) *Plant Cell* **17,** 204–218
15. Aluri, S., and Büttner, M. (2007) *Proc. Natl. Acad. Sci. U.S.A.* **104,** 2537–2542
16. Toyofuku, K., Kasahara, M., and Yamaguchi, J. (2000) *Plant Cell Physiol.* **41,** 940–947
17. Barth, I., Meyer, S., and Sauer, N. (2003) *Plant Cell* **15,** 1375–1385
18. Weise, A., Barker, L., Kühn, C., Lalonde, S., Buschmann, H., Frommer, W. B., and Ward, J. M. (2000) *Plant Cell* **12,** 1345–1355
19. Büttner, M. (2007) *FEBS Lett.* **581,** 2318–2324
20. Kiyosue, T., Yamaguchi-Shinozaki, K., and Shinozaki, K. (1994) *Plant Mol. Biol.* **25,** 791–798
21. Osakabe, Y., Maruyama, K., Seki, M., Satou, M., Shinozaki, K., and Yamaguchi-Shinozaki, K. (2005) *Plant Cell* **17,** 1105–1119
22. Sakuma, Y., Maruyama, K., Osakabe, Y., Qin, F., Seki, M., Shinozaki, K., and Yamaguchi-Shinozaki, K. (2006) *Plant Cell* **18,** 1292–1309
23. Qin, F., Sakuma, Y., Tran, L. S., Maruyama, K., Kidokoro, S., Fujita, Y., Fujita, M., Umezawa, T., Sawano, Y., Miyazono, K., Tanokura, M., Shinozaki, K., and Yamaguchi-Shinozaki, K. (2008) *Plant Cell* **20,** 1693–1707
24. Mizuno, S., Osakabe, Y., Maruyama, K., Ito, T., Osakabe, K., Sato, T., Shinozaki, K., and Yamaguchi-Shinozaki, K. (2007) *Plant J.* **50,** 751–766
25. Yoo, S. D., Cho, Y. H., and Sheen, J. (2007) *Nat. Protoc.* **2,** 1565–1572
26. Matsuoka, K., and Nakamura, K. (1991) *Proc. Natl. Acad. Sci. U.S.A.* **88,** 834–838
27. Petrásek, J., Mravec, J., Bouchard, R., Blakeslee, J. J., Abas, M., Seifertová, D., Wisniewska, J., Tadele, Z., Kubes, M., Covanová, M., Dhonukshe, P., Skupa, P., Benková, E., Perry, L., Krecek, P., Lee, O. R., Fink, G. R., Geisler, M., Murphy, A. S., Luschnig, C., Zazímalová, E., and Friml, J. (2006) *Science* **312,** 914–918
28. Ohyama, A., Ito, H., Sato, T., Nishimura, S., Imai, T., and Hirai, M. (1995) *Plant Cell Physiol.* **36,** 369–376
29. Tang, X., Ruffner, H. P., Scholes, J. D., and Rolfe, S. A. (1996) *Planta* **198,** 17–23
30. Chiou, T. J., and Bush, D. R. (1996) *Plant Physiol.* **110,** 511–520
31. Uldry, M., and Thorens, B. (2004) *Pflugers Arch.* **447,** 480–489
32. Kiyosue, T., Abe, H., Yamaguchi-Shinozaki, K., and Shinozaki, K. (1998) *Biochim. Biophys. Acta* **1370,** 187–191
33. Meyer, S., Lauterbach, C., Niedermeier, M., Barth, I., Sjolund, R. D., and Sauer, N. (2004) *Plant Physiol.* **134,** 684–693
34. Yamaguchi-Shinozaki, K., and Shinozaki, K. (2006) *Annu. Rev. Plant Biol.* **57,** 781–803
35. Augustin, R., Riley, J., and Moley, K. H. (2005) *Traffic* **6,** 1196–1212
36. Ibberson, M., Uldry, M., and Thorens, B. (2000) *J. Biol. Chem.* **275,** 4607–4612
37. Ueda, T., Yamaguchi, M., Uchimiya, H., and Nakano, A. (2001) *EMBO J.* **20,** 4730–4741
38. Jaillais, Y., Fobis-Loisy, I., Miège, C., and Gaude, T. (2008) *Plant J.* **53,** 237–247
39. Roitsch, T., and González, M. C. (2004) *Trends Plant Sci.* **9,** 606–613
40. Haouazine-Takvorian, N., Tymowska-Lalanne, Z., Takvorian, A., Tregear, J., Lejeune, B., Lecharny, A., and Kreis, M. (1997) *Gene* **197,** 239–251
41. Reinders, A., Panshyshyn, J. A., and Ward, J. M. (2005) *J. Biol. Chem.* **280,** 1594–1602
42. Pelleschi, S., Guy, S., Kim, J. Y., Pointe, C., Mahé, A., Barthes, L., Leonardi, A., and Prioul, J. L. (1999) *Plant Mol. Biol.* **39,** 373–380
43. Trouverie, J., Chateau-Joubert, S., Thévenot, C., Jacquemot, M. P., and Prioul, J. L. (2004) *Planta* **219,** 894–905
44. Huang, S., and Czech, M. P. (2007) *Cell Metabolism* **5,** 237–252
45. Bonifacino, J. S., and Traub, L. M. (2003) *Annu. Rev. Biochem.* **72,** 395–447
46. Janvier, K., Kato, Y., Boehm, M., Rose, J. R., Martina, J. A., Kim, B. Y., Venkatesan, S., and Bonifacino, J. S. (2003) *J. Cell Biol.* **163,** 1281–1290